J. Inst. Eng. India Ser. D
https://doi.org/10.1007/s40033-024-00757-x

ORIGINAL CONTRIBUTION

Investigations on the Effect of Heat Treatment on Wear Behavior and Structure of Inconel 713 Alloy

Vinayak P. Suryawanshi[1] · **Prashant D. Deshmukh**[1]

Received: 25 February 2024 / Accepted: 2 May 2024

Abstract In this study, tribological wear and Brinell hardness number characteristics of Inconel 713 alloy in its as-received state, following heat treatment was explored. The investigation focused on the effects of heat treatment at temperatures of −140 °C and −196 °C for durations of 24, 36, and 48 h using DCT Process. At room temperature, Inconel 713 alloy maintains a stable γ phase with a face-centered cubic (FCC) structure, which imparts excellent mechanical properties along with corrosion and oxidation resistance. However, despite its commendable mechanical traits, the alloy demonstrates insufficient wear resistance in cutting tool applications, prompting a quest for enhanced wear properties. Thus, this study endeavors to improve wear resistance by subjecting the specimen to a heat treatment environment, facilitating the transformation from austenite to martensite without embrittlement. Through comprehensive analysis, including examination of microstructure, wear behavior, and hardness, we aim to elucidate the alloy's performance under these conditions.

Keywords Inconel 713 superalloy · Wear · Hardness · Heat treatment

✉ Vinayak P. Suryawanshi
vsuryawanshi0591@gmail.com

Prashant D. Deshmukh
pddeshmukh7@gmail.com

[1] Department of Mechanical Engineering, Datta Meghe College of Engineering, Airoli, Navi Mumbai 400708, India

Introduction

Inconel 713 alloy represents a class of nickel-based superalloys renowned for their exceptional high-temperature strength, corrosion resistance, and mechanical properties [1–3]. Developed primarily for use in demanding aerospace and gas turbine engine applications, Inconel 713 has become synonymous with reliability in extreme environments. Engineered with a precise balance of nickel, chromium, aluminum, and other alloying elements, Inconel 713 exhibits remarkable resistance to oxidation and high-temperature degradation [4–7]. Its robustness at elevated temperatures makes it a preferred material for components exposed to extreme heat and stress, such as turbine blades, combustion chambers, and exhaust systems [4, 8, 9]. The alloy's microstructure, characterized by a stable γ (gamma) phase with a face-centered cubic (FCC) crystal lattice, contributes to its superior mechanical integrity and resistance to creep and fatigue [1, 10–13]. Additionally, Inconel 713 maintains its strength and performance across a wide range of temperatures, ensuring reliability in the most challenging operational conditions. Inconel 713's versatility extends beyond aerospace to encompass various industrial sectors where high-performance materials are essential [14–18]. Its ability to withstand harsh environments while maintaining structural integrity makes it indispensable in applications where durability and longevity are paramount.

However, some challenges exist and needs addressing by the scientific community, few to name uneconomical i.e., they are too costly and can be accommodated only to specific limited applications [11, 19–21]. They lack property of weldability due to its high nickel content and other constituent compositions resulting in cracking [22]. Inconel 713 alloy is known for its poor machinability compared to conventional steels [23]. Its high strength and toughness

Published online: 13 May 2024

make it difficult to machine, leading to increased tool wear, reduced cutting speeds, and lower machining efficiency [24, 25]. Specialized machining techniques and tooling are often required, adding to manufacturing expenses. While Inconel 713 alloy maintains excellent mechanical properties at high temperatures, it may become brittle at low temperatures [26]. This can limit its suitability for cryogenic applications where materials need to withstand extreme cold without becoming brittle or susceptible to fracture.

To surmount the above challenges, there have been substantial literature cited in the scientific text that discourses various pre and post heat treatment procedures, various processing routes to resolve these challenges. A decent literature on various processing methodologies such as powder metallurgical process that involves conventional melting, casting, forging [27], machining and surface treatment were found to be most widely used methods. However, due to advent of the technologies, recently additive manufacturing techniques have also been reported in a decent magnitude in the scientific community [28, 29]. However, each of these methods have their advantages and disadvantages, as a result, a more rigorous studies have been investigated for various other Inconel alloys subjected to various post heat treatment procedures. One such potential solution that is widely recognized is subjecting the materials to the extremely low temperatures referred to as cryogenic temperatures to a maximum range of −150 °C [30]. From the literature, it can be pursued that, the cryogenic treatment of the Inconel enhances the stabilization of the microstructure i.e., reduces residual stress induced due to processing at high temperatures and post heat treatments followed also it will promote the formation of the finer and uniform grain structures along the grain boundaries thus enhancing the mechanical strength and toughness [31, 32]. Transformation of austenite to martensite enhances the hardness and wear resistance due to the re-arrangement of the atoms within the crystal structure along various planes [33–35]. Reduction of retained austenite phase enhances the harness of the material and thus increasing the amenability towards the improved machinability, this is attributed to the transformation of reduced austenite to a stable martensite phase [36–38]. Lastly enhanced wear resistance and improved dimensional stability can be achieved when treated at cryogenic environments [39–42].

Hence in the current work, we investigate the as received Inconel 713 alloy for its tribological wear, hardness and microstructural characteristics. Followed by further subjected to the specimen to the cryogenic temperatures i.e., −140 °C and −190 °C for 24,36 and 48 h for seven number of samples for hardness, and seven number of samples for wear rate and average of three is noted. Further, we have established a structure–property correlation at the end of the section in brief.

Materials and Methodology

Cryogenic Treatment

In the current work, procedure for the cryogenic treatment was performed at Arctic Cryogenics, Pune. The machine used has a capability of maintaining the cryogenic temperatures around −196 °C. The cryogenic furnace can complete the cryogenic treatment of the specimen without any embrittlement from austenite to martensite and with machine completely automated. The re-arrangement of the atoms from FCC to cubic tetragonal can be achieved. The process involves the soaking of the specimens in the liquid nitrogen (LN2) and the temperature rate is fixed to decrease 1 °C/minute until the desired temperatures of −140 °C and −196 °C are achieved. Further the soaking time was presumed to be 24, 36 and 48 h to finish the complete process of the martensite temperature range. The following Fig. 1 depicts the cryogenic furnace used in the current experiment.

The as received samples were then surface finished for further characterizations such as wear, hardness and the microstructural characterization through wire EDM process to get the desired sample geometries. The work piece, which is the cryogenically treated Inconel 713, is mounted on the EDM machine. The machine's settings, including the wire tension, power settings, and flushing parameters, are adjusted according to the requirements of the job. Following which the following specimens were displayed in the Fig. 2 below.

Fig. 1 Cryogenic treatment equipment

Fig. 2 Samples during cryogenic treatment

Fig. 3 Tribological wear testing machine (Pin-on-disk setup)

Fig. 4 Brinell Hardness tester setup for Hardness Evaluation

Material Characterization

There were fourteen samples prepared in total for both sets individually to characterize for the hardness, wear rate and microstructural properties. Initially the specimens were characterized for tribological wear resistance using pin-on-disk setup as displayed in the Fig. 3. The wear rate is characterized for all the samples at constant rpm of 500 rpm at 8 kg load for 30 min with counter face hardened EN8. EN8 is a medium carbon steel grade commonly used in various engineering applications due to its good machinability, wear resistance, and toughness properties (52HRC). The diameter of the sample $12 \times 25 \times 30$ mm [43–46].

Hardness testing is performed on Brinell hardness to identify the Brinell hardness number (BHN) and the same machine can be referred in the Fig. 4 below. The process of the evaluation of the BHN involves the preparation of the specimen which includes the surface finishing ensuring that it is clean. The load at which the testing is performed is 150 kg with a

dwell time of 20 s. The BHN was then calculated using the formulae

$$HB = \frac{2 * load}{\pi * diameter * (Diameter - \sqrt{diameter^2 - Indentationdiameter^2})}$$

Further microstructural characterization is performed on the wear sample for using scanning electron microscopy to identify the arrangement of the grain boundaries and grain refinement mechanism. The surface morphology of the wear samples was using to corroborate the study of the different phases using the crystallographic data the mechanical and tribological characteristics. Further, for the same materials X-Ray Diffraction for the identification of the crystallographic phases was identified for both treated and untreated sample. The XRD confirms the presence of the crystal phase and will be able to provide the information of the microstructural transformation to corroborate the studies of the mechanical and tribological characteristics. A detailed investigation is reported in the following results and discussion section.

Results and Discussion

Correlation of Specific Wear Rate and Hardness After Treatment

The samples were initially characterized for the tribological wear resistance for all the ten samples, out of the ten samples for each of the conditions, the average for the each of the specimens for the conditions as discussed earlier was reported. The conditions used are temperature ranges −140 °C and −196 °C for 24, 36 and 48 h. The wear results for the same can be inferred in Table 1 as follows. It can have realized that for temperature ranges of −196 °C for 48 h was found to be the best sample as it has displayed excellent sliding wear resistance of $13.98*10^{-7}$ mm^3/min, compared to the same for −140 °C. It can also be observed that, there is transition of the crystal planes which actually reduced the sliding wear resistance indicating further the transformation possible for suitability for enhancing sliding wear resistance. The untreated and treated at −196 °C indicate enhanced wear resistance also indicating reduction in austenite phase. The lowest sliding wear rate was observed at 36 h at −140 °C.

Table 1 Sliding wear resistance of treated and untreated samples

Sl. no	Temperature	Time of soaking	Sliding wear resistance (mm^3/min)
1	Untreated	No soaking	$8.87*10^{-7}$
2	−140 °C	24 h	$4.47*10^{-7}$
		36 h	$2.51*10^{-7}$
		48 h	$4.46*10^{-7}$
3	−196 °C	24 h	$3.68*10^{-7}$
		36 h	$6.70*10^{-7}$
		48 h	$13.98*10^{-7}$

The HRB_{100} for the treated and untreated samples for various time of soaking have displayed in the table. For various soaking time and the temperature ranges, we have identified that at -196 °C for 48 h has displayed the peak hardness number of 89 and with lowest of untreated at 70 as reported in Table 2. However, the soaking has been improved the crystal phase transformation by reducing the austenite phase

Table 2 Hardness number for treated and untreated sample

Sl. no	Temperature	Time of soaking	HRB_{100}
1	Untreated	No soaking	70
2	−140 °C	24 h	70
		36 h	76
		48 h	83
3	−196 °C	24 h	85
		36 h	88
		48 h	89

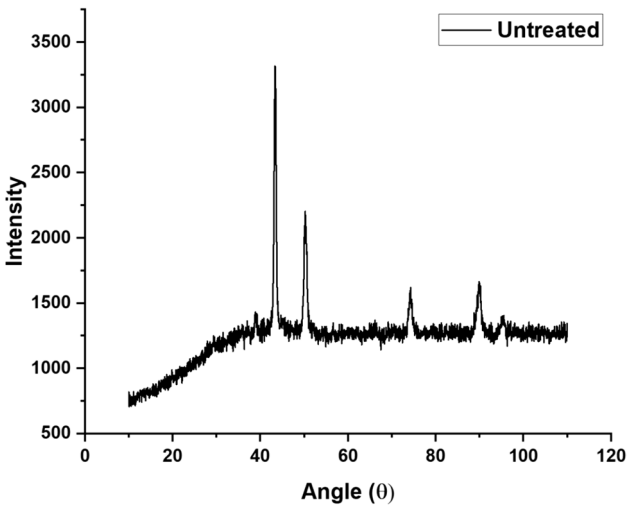

Fig. 5 XRD peaks of untreated Inconel 713 sample

this allowing the grain boundaries to rearrange themselves to a phase that enhances the hardness of the material. But further increment in the soaking time and temperature may transform the crystal structure or new phase that can reduce the hardness. Thus, it is also important to identify the temperature and soaking time which is crucial for enhancing the wear and hardness properties.

The XRD crystallography for the treated and untreated samples of the Inconel 713 has been displayed below in Fig. 5. The γ phase in the figure displays (111), (200), (220), (311), (420) for an untreated Inconel 713. The (111) is the face centered cubic structure at θ = 41.2 °C and (2 0 0) with high intensity reflecting the overall crystal structure of the specimen and (2 2 0) indicating the crystal planes and hence the Inconel 713 in its untreated form exhibit excellent mechanicals strength. At the same time, γ' phase indicating the strengthening mechanism. Whereas when the same is treated at −140 °C, it can be observed that there is reduction in the austenite phase and hence the intensity of the peak changes and this change can be observed in the following Fig. 6 thus attributing towards orientation of the crystal phase. At the same time martensite phase is also found to be enhanced without embrittlement resulting in the enhanced wear resistance [47–51].

In a similar context, when further the temperature is increased to −196 °C has displayed a sharp presence of austenite phase at 24 h, but over the increment in the soaking time, the residual stresses have completely been reduced or mostly reducing thus resulting in the reduction of the austenite phase and attributing towards complete martensitic phase thus attributing to the rearrangements of the atoms within

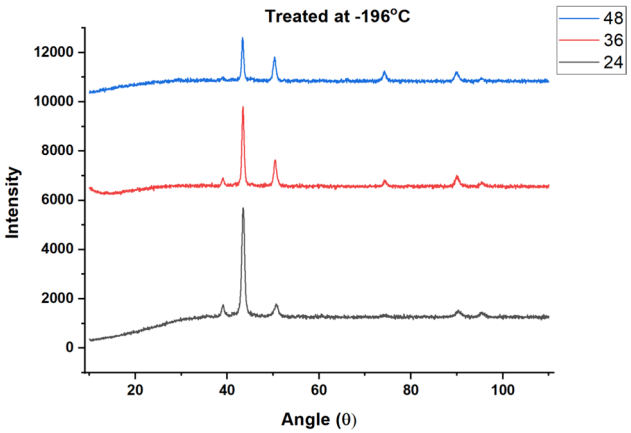

Fig. 7 XRD peaks of treated Inconel 713 sample at −196 °C

the crystal structure along the various planes as can be seen in Fig. 7. This mechanism enhances the tribological wear and hardness of the specimen and the same can be inferred from the results of tribology and mechanical characteristics [52–54]. It can be also inferred that; the peak broadening can be observed in (200) plane indicating the presence of the smaller grain sizes. The low temperatures must have accelerated the precipitation of fine carbides and other secondary phases, introduced additional peaks or modified existing ones. One of the interesting aspects is, we haven't seen drastic peak variations because of the low rate of temperature i.e., 1°/min. Similar context, as the soaking time increased the phase transformation and degree of peak started to alter.

Fig. 6 XRD peaks of treated Inconel 713 sample at −140 °C

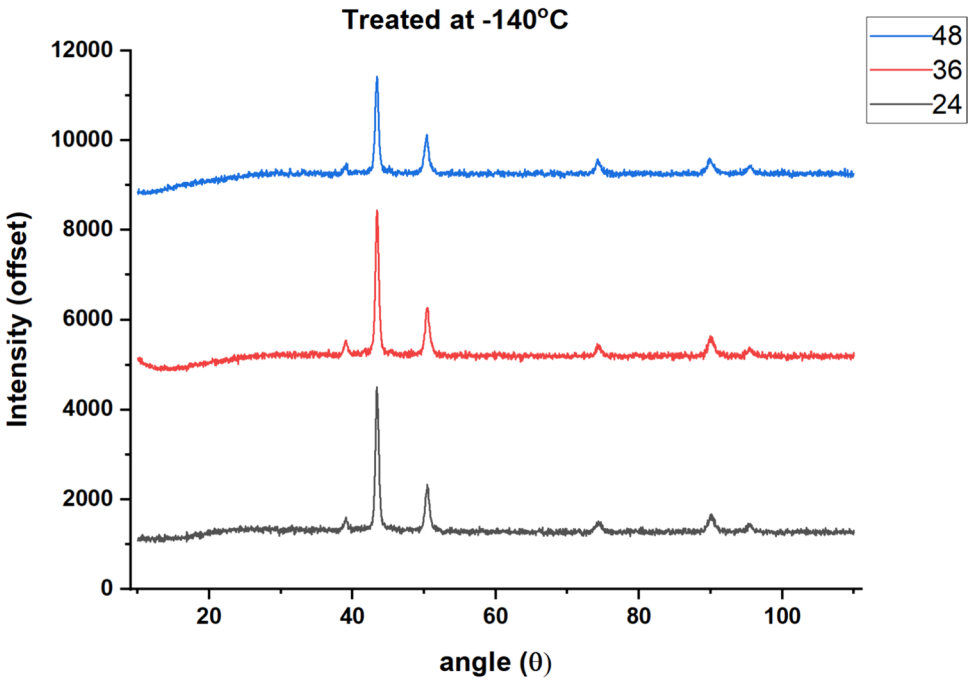

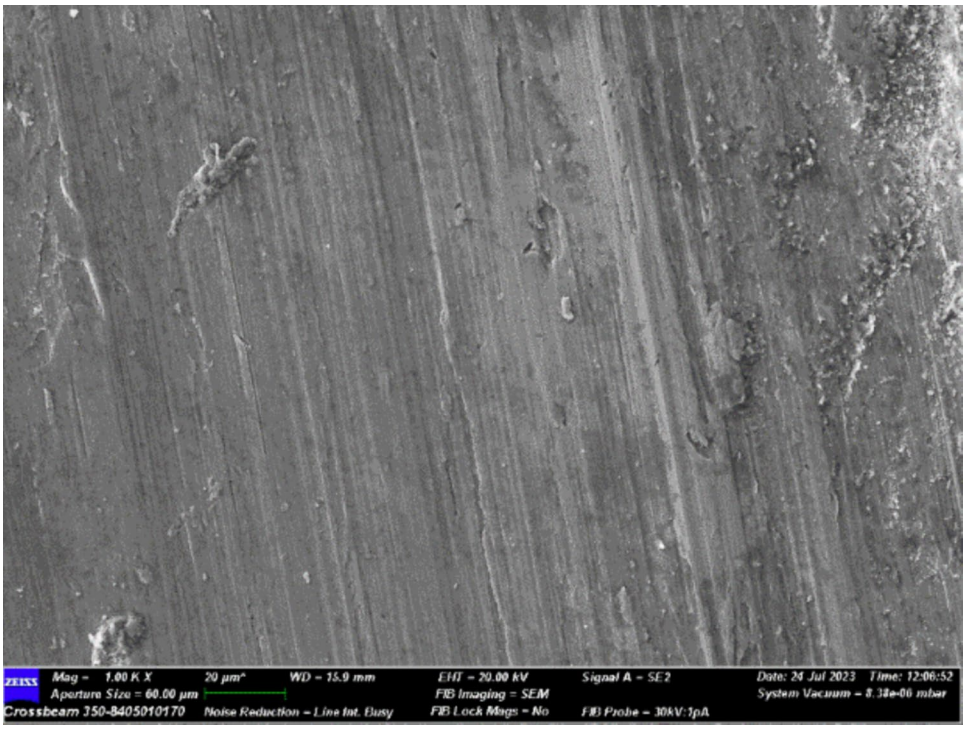

Fig. 8 SEM of untreated Inconel 713 wear sample

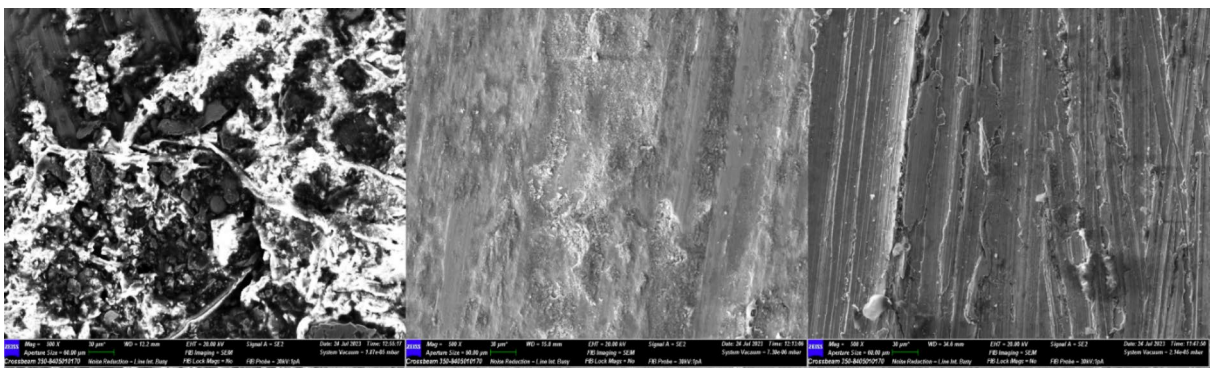

Fig. 9 SEM micrography of treated Inconel 713 sample at −140 °C

The following Fig. 8 displays the untreated Inconel 713 alloys subjected to tribological wear and it can be understood that the material exhibited the FCC γ nickel matrix with γ' intermetallic precipitates. The wear properties completely depend on the size, shape and distribution of γ' intermetallic precipitates. It can be corroborated that the enhancement of the wear resistance is attributed to the uniform shape and size of the γ' intermetallic precipitates followed the increased γ' intermetallic precipitates size as shown int the figure. As the temperature is decreasing further, a fine grain structures have been evolved as can be observed in the Figs. 8 and 9 below. But it must also be taken care that the increase in the cryogenic exposure will lead to ductile–brittle transition and material may tend to fail in brittle fracture.

The Fig. 9 displays the wear structures indicating that residual stresses stabilizing the surface microstructure of alloy, making them more resistant to phase transformations and microstructural changes that occur during wear processes. This stability helps maintain the material's integrity and mechanical properties, prolonging its wear life. The Fig. 10 displays the perfect structure with small craters that can be observed indicating the absence of complete ternary alloys and reduced stress relaxation due to larger soaking time resulting in surface cracks. It may also be extrapolated that cryogenic treatment affects the texture of titanium alloys as well as the distribution of crystallographic orientations inside the material. An unfavourable texture distribution can result in anisotropic mechanical characteristics, in which the

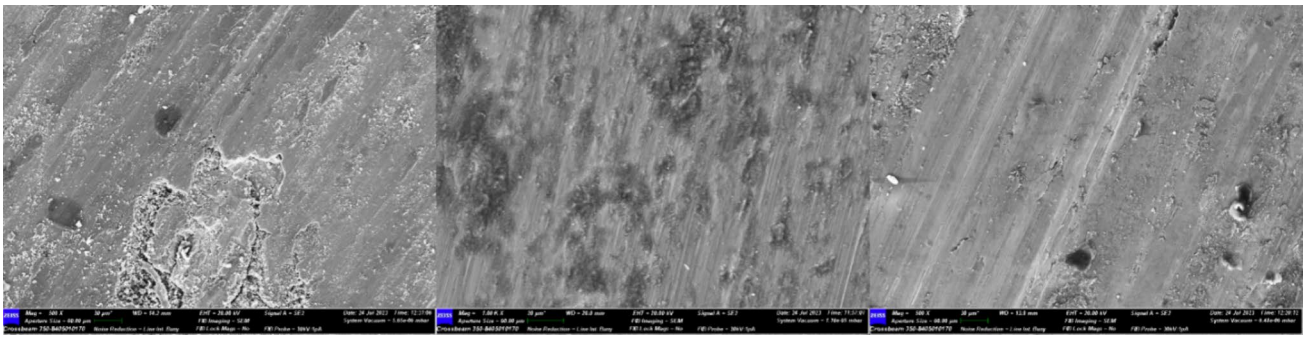

Fig. 10 SEM micrography of treated Inconel 713 sample at −196 °C

material has varying strengths and ductility in various directions. These residual stresses can cause localised regions of high stress concentration, making the material more prone to brittle fracture, especially under applied pressures.

Conclusions

The current work found that there is a substantial enhancement in the sliding wear resistance and hardness in the samples when subjected to the cryogenic treatment. The parameters used in the cryogenic treatment i.e., soaking time and temperature have showed significant effect on the mechanical hardness and tribological wear properties. It is also evidential that there is a reduction in the structural phase of the material to the martensite very clearly from the XRD crystallography as result of reduction in the peak size attributing towards the reduction of austenite state and increment in the stable martensitic γ phase. This is intriguing that the residual stress also reduced ensuing that the stress relaxation process has been induced increment in the tribological wear which can be observed as a craters in the SEM micrographs. Overall, cryogenic treatment can have significant positive effects on the surface stability of materials by promoting the formation of a more stable microstructure, reducing residual stresses, enhancing wear resistance, and improving dimensional stability.

Funding The authors have not disclosed any funding.

Data Availability The data used to support the findings of this study are included within the article. Further data or information is available from the corresponding author upon request.

Declarations

Conflict of interest The authors have not disclosed any competing interests.

References

1. P. Jonsta, Z. Jonsta, J. Sojka, L. Cizek, A. Hernas, Structural characteristics of nickel super alloy INCONEL 713LC after heat treatment. J. Achiev. Mater. Manuf. Eng. **21**(2), 29–32 (2007)
2. L. Kunz, P. Lukáš, R. Konečná, High-cycle fatigue of Ni-base superalloy Inconel 713LC. Int. J. Fatigue **32**(6), 908–913 (2010)
3. D.B. Lee, High-temperature oxidation of Ni-based Inconel 713 alloys at 800–1100℃ in air. J. Korean Inst. Surf. Eng. **44**(5), 196–200 (2011)
4. K. Łyczkowska et al., Properties of the Inconel 713 Alloy within the high temperature brittleness range. Arch. Foundry Eng. 17 (2017)
5. R.R. Boyer, J.D. Cotton, M. Mohaghegh, R.E. Schafrik, Materials considerations for aerospace applications. MRS Bull. **40**(12), 1055–1066 (2015)
6. P.P. Raut, A.S. Rao, S. Sollapur et al., Investigation on the development and building of a voice coil actuator-driven XY micromotion stage with dual-range capabilities. Int. J. Interact. Des. Manuf. (2023). https://doi.org/10.1007/s12008-023-01665-2
7. O.B. Loureda, J.O. Gomes, W. Vireira, Analysis about Machinability of Superalloys applied on Turbines of LRE Turbopumps. in *49th AIAA/ASME/SAE/ASEE Joint PropulsionConference* (2013), p. 4067
8. K.B.S. Rao, H.P. Meurer, H. Schuster, Creep-fatigue interaction of Inconel 617 at 950 C in simulated nuclear reactor helium. Mater. Sci. Eng. A **104**, 37–51 (1988)
9. Inconel-713LC gas turbine blades. Mater. Sci. Eng.: A. **642**, 230–240
10. S. Dehghan, E. Soury, A comparative study on machining and tool performance in friction drilling of difficult-to-machine materials AISI304, Ti-6Al-4V, Inconel718. J. Manuf. Process. **61**, 128–152 (2021)
11. V.G. Sanap, V.D. Shinde, Machinability improvement of Inconel 718 during heat treatment-A review. in *Journal of Physics: Conference Series*, vol. 1706, no. 1 (2020), p. 012175. IOP Publishing
12. G.R. Chate et al., Ceramic material coatings: emerging future applications. in *Advanced Ceramic Coatings for Emerging Applications* (Elsevier, 2023). pp 3–17. https://doi.org/10.1016/B978-0-323-99624-2.00007-3
13. B.K. Yoo, H.K. Choi, H.I. Park, H.Y. Jeong, The Effect of Heat Treatment on the microstructures and mechanical properties of Inconel 713C alloy vacuum investment castings. J. Korea Foundry Soc. **40**(2), 16–24 (2020)
14. P.G. Bedmutha, P.M. Waghmare, S.B. Sollapur, Mechanical properties of bamboo fiber reinforced plastics. Int. J. Sci. Adv. Res. Technol. **3**(9), 365–368 (2017)

15. S. Sollapur, M.S. Patil, K. Chaporkar, A. Misal, R. Bhoyar, K. Dhole, Design and Development of Constrain Based XY Flexural Mechanism, in *Techno-Societal 2018*. ed. by P. Pawar, B. Ronge, R. Balasubramaniam, A. Vibhute, S. Apte (Springer, Cham, 2020). https://doi.org/10.1007/978-3-030-16962-6_27
16. J.R. Zhao, F.Y. Hung, C.S. Lu, I.C. Lai, Comparison of laser powder bed fusion and cast Inconel 713 alloy in terms of their microstructure, mechanical properties, and fatigue life. Adv. Eng. Mater. **23**(6), 2001366 (2021)
17. M. Lachowicz, W. Dudziński, K. Haimann, M. Podrez-Radziszewska, Microstructure transformations and cracking in the matrix of γ–γ′ superalloy Inconel 713C melted with electron beam. Mater. Sci. Eng. A **479**(1–2), 269–276 (2008)
18. K. Wu, S.W. Chee, W. Sun, A.W.Y. Tan, S.C. Tan, E. Liu, W. Zhou, Inconel 713C coating by cold spray for surface enhancement of Inconel 718. Metals **11**(12), 2048 (2021)
19. M. Godec, S. Malej, D. Feizpour, Č Donik, M. Balažic, D. Klobčar, L. Pambaguian, M. Conradi, A. Kocijan, Hybrid additive manufacturing of Inconel 718 for future space applications. Mater CharactCharact. **172**, 110842 (2021)
20. D.D. Baviskar, A.S. Rao, S. Sollapur et al., Development and testing of XY stage compliant mechanism. Int. J. Interact. Des. Manuf. (2023). https://doi.org/10.1007/s12008-023-01612-1
21. J. Schneider, L. Farris, G. Nolze, S. Reinsch, G. Cios, T. Tokarski, S. Thompson, Microstructure evolution in Inconel 718 produced by powder bed fusion additive manufacturing. J. Manuf. Mater. Proc. **6**(1), 20 (2022)
22. P. Waghmare, Development and Performance Investigation of Solar Concrete Collector at Different Climatic Conditions. Indian J. Eng. Mater. Sci. (2023). https://doi.org/10.56042/ijems.v30i2.1384
23. S.L. Chittewar, N.G. Patil, Surface integrity of conventional and additively manufactured nickel superalloys: a review. Mater Today: Proc. **44**, 701–708 (2021)
24. D. Deng, *Additively Manufactured Inconel 718: Microstructures and Mechanical Properties (vol. 1798)* (Linköping University Electronic Press, Linköping, 2018)
25. I.S. Jawahir, H. Attia, D. Biermann, J. Duflou, F. Klocke, D. Meyer, S.T. Newman, F. Pusavec, M. Putz, J. Rech, V. Schulze, Cryogenic manufacturing processes. CIRP Ann. **65**(2), 713–736 (2016)
26. S. Sollapur, D. Saravanan et al., Tribological properties of filler and green filler reinforced polymer composites. Mater. Today: Proc. **50**, 2065–2072 (2022). https://doi.org/10.1016/j.matpr.2021.09.414
27. K.P. Toradmal, P.M. Waghmare, S.B. Sollapur, Three point bending analysis of honeycomb sandwich panels: experimental approach. Int. J. Eng. Tech. **3**(5), 1–5 (2017)
28. U.A. Khilare, S.B. Sollapur, Investigation of residual stresses and its effect on mechanical behaviour of AISI310. J. Res. **2**(5), 42–46 (2016) ISSN: 2395-7549
29. B. Gireesh, B. SollapurShrishail, V.N. Satwik, Finite element & experimental investigation of composite torsion shaft. Int. J. Engg. Res. Appl. **3**(2), 1510–1517 (2013)
30. K. Łyczkowska, J. Adamiec, The phenomena and criteria determining the cracking susceptibility of repair padding welds of the Inconel 713C Nickel Alloy. Materials **15**(2), 634 (2022)
31. C. Durga Prasad, S. Joladarashi, M.R. Ramesh, M.S. Srinath, B.H. Channabasappa, Comparison of high temperature wear behavior of microwave assisted HVOF sprayed CoMoCrSi-WC-CrC-Ni/WC-12Co composite coatings. Silicon, Springer **12**, 3027–3045 (2020). https://doi.org/10.1007/s12633-020-00398-1
32. A. Chamanfar, M. Jahazi, A. Bonakdar, E. Morin, A. Firoozrai, Cracking in fusion zone and heat affected zone of electron beam welded Inconel-713LC gas turbine blades. Mater. Sci. Eng. A **642**, 230–240 (2015)
33. P.M. Waghmare, P.G. Bedmutha, S.B. Sollapur, Investigation of effect of hybridization and layering patterns on mechanical properties of banana and kenaf fibers reinforced epoxy biocomposite. Mater. Today: Proc. **46**, 3220–3224 (2021). https://doi.org/10.1016/j.matpr.2020.11.194
34. T. Shinde et al., Fatigue analysis of alloy wheel using cornering fatigue test and its weight optimization. Mater. Today: Proc. **62**, 1470–1474 (2022). https://doi.org/10.1016/j.matpr.2022.02.023
35. M. Vinod, C.A. Kumar, S.B. Sollapur et al., Study on fabrication and mechanical performance of flax fibre-reinforced aluminium 6082 laminates. J. Inst. Eng. India Ser. D. (2023). https://doi.org/10.1007/s40033-023-00605-4
36. C. Durga Prasad, A. Jerri, M.R. Ramesh, Characterization and sliding wear behavior of iron based metallic coating deposited by HVOF process on low carbon steel substrate. J Bio- Tribo-Corros., Springer (2020). https://doi.org/10.1007/s40735-020-00366-7
37. S.S. Shinde, S.B. Sollapur, Effect of Residual Stress on the Mechanical Behavior of AISI 304, For TIG Welding. in *International Journal of Scientific & Engineering Research,* vol 8, no. 10, October 2017
38. C. Durga Prasad, S. Joladarashi, M.R. Ramesh, M.S. Srinath, Microstructure and tribological resistance of flame sprayed CoMoCrSi/WC-CrC-Ni and CoMoCrSi/WC-12Co composite coatings remelted by microwave hybrid heating. J. Bio-Tribo-Corros., Springer **6**, 124 (2020). https://doi.org/10.1007/s40735-020-00421-3
39. C. Venkate Gowda, T.K. Nagaraja, K.B. Yogesha et al., Study on structural behavior of HVOF-Sprayed NiCr/Mo coating. J. Inst. Eng. India Ser. D. (2024). https://doi.org/10.1007/s40033-024-00641-8
40. S.B. Sollapur, P.C. Sharath, P. Waghmare, Applications of Additive Manufacturing in Biomedical and Sports Industry, in *Practical Implementations of Additive Manufacturing Technologies. Materials Horizons: From Nature to Nanomaterials*. ed. by S. Rajendrachari (Springer, Singapore, 2024). https://doi.org/10.1007/978-981-99-5949-5_13
41. C. Durga Prasad, S. Joladarashi, M.R. Ramesh, M.S. Srinath, B.H. Channabasappa, Influence of microwave hybrid heating on the sliding wear behaviour of HVOF sprayed CoMoCrSi coating. Mater. Res. Express, IOP **5**, 086519 (2018). https://doi.org/10.1088/2053-1591/aad44e
42. S. Sollapur, T. Shinde, S. Raut, A. Atpadkar, P. Nimbalkar, M. Rathod, Design and Development of High-Precision Scanning Flexural Mechanism Using PID, in *Recent Advances in Operations Management and Optimization. CPIE 2023. Lecture Notes in Mechanical Engineering*. ed. by A. Sachdeva, K.K. Goyal, R.K. Garg, J.P. Davim (Springer, Singapore, 2024). https://doi.org/10.1007/978-981-99-7445-0_4
43. Y. Yildiz, M. Nalbant, A review of cryogenic cooling in machining processes. Int. J. Mach. Tools Manuf **48**(9), 947–964 (2008)
44. R.N. Chikkangoudar, C. Patil, R.N. Panchal et al., Investigating joint-free mechanical systems with PLA and ABS materials using the fuse deposition modelling method. J. Inst. Eng. India Ser. D. (2024). https://doi.org/10.1007/s40033-024-00659-y
45. C. Durga Prasad, S. Joladarashi, M.R. Ramesh, M.S. Srinath, B.H. Channabasappa, Effect of microwave heating on microstructure and elevated temperature adhesive wear behavior of HVOF deposited CoMoCrSi-Cr_3C_2 composite coating. Surf. Coatings Technol, Elsevier Sci. **374**, 291–304 (2019). https://doi.org/10.1016/j.surfcoat.2019.05.056
46. C. Durga Prasad, S. Joladarashi, M.R. Ramesh, M.S. Srinath, B.H. Channabasappa, Microstructure and tribological behavior of flame sprayed and microwave fused CoMoCrSi/CoMoCrSi-Cr_3C_2 coatings. Mater. Res. Express, IOP **6**(2019). https://doi.org/10.1088/2053-1591/aaebd9

47. M. Vinod, C.A. Kumar, S.B. Sollapur et al., Study on Low-Velocity Impact Performance of Chemical Treated Flax Fibre-Reinforced Aluminium 6082 Laminates. J. Inst. Eng. India Ser. D. (2024). https://doi.org/10.1007/s40033-024-00657-0
48. U.M.R. Paturi, N.S. Reddy, Progress of machinability on the machining of Inconel 718: a comprehensive review on the perception of cleaner machining. Clean. Eng. Technol. **5**, 100323 (2021)
49. N.G. Siddeshkumar, R. Suresh, C. Durga Prasad, L. Shivaram, N.H. Siddalingaswamy, Evolution of the surface quality and tool wear in the high speed turning of Al2219/n-B4C/MoS_2 metal matrix composites. Int. J. Cast Met. Res., Taylor Francis. (2023). https://doi.org/10.1080/13640461.2023.2285177
50. C. Durga Prasad, S. Kollur, C.R. Aprameya, T.V. Chandramouli, T. Jagadeesha, B.N. Prashanth, Investigations on tribological and microstructure characteristics of WC-12Co/FeNiCrMo composite coating by HVOF process. JOM J. Miner., Met. Mater. Soc. (TMS), Springer (2023). https://doi.org/10.1007/s11837-023-06242-2
51. S. Gotagunaki, V.S. Mudakappanavar, R. Suresh, C. Durga Prasad, Studies on the mechanical properties and wear behavior of an AZ91D magnesium metal matrix composite utilizing the stir casting method. Metallogr., Microstruct., Anal., Springer. (2023). https://doi.org/10.1007/s13632-023-01017-2
52. C. Durga Prasad, S. Kollur, M. Nusrathulla, G. SatheeshBabu, M.B. Hanamantraygouda, B.N. Prashanth, N. Nagabhushana, Characterisation and wear behaviour of SiC reinforced FeNiCrMo composite coating by HVOF process. Trans. IMF, Taylor Francis, (2023). https://doi.org/10.1080/00202967.2023.2246259
53. T. Naik, C. MahantayyaMathapathi, D. Prasad, H.S. Nithin, M.R. Ramesh, Effect of laser post treatment on microstructural and sliding wear behavior of HVOF sprayed NiCrC and NiCrSi coatings. Surf. Rev. Lett. **29**(1), 225000 (2022). https://doi.org/10.1142/S0218625X2250007X
54. C. Durga Prasad, S. Lingappa, M.R. SharnappaJoladarashi, S.B. Ramesh, Characterization and sliding wear behavior of CoMoCrSi+Flyash composite cladding processed by Microwave irradiation. Mater. Today Proc., Elsevier Sci. **46**, 2387–2391 (2021). https://doi.org/10.1016/j.matpr.2021.01.156